



HAL
open science

Development of an in-situ measurement device for airfield pavement interface characterization

Maissa Gharbi, Michaël Broutin, Jean-Marie Roussel, Armelle Chabot

► To cite this version:

Maissa Gharbi, Michaël Broutin, Jean-Marie Roussel, Armelle Chabot. Development of an in-situ measurement device for airfield pavement interface characterization. *Journal of Testing and Evaluation*, 2022, 50 (2), pp.818-835. 10.1520/JTE20210211 . hal-03475362

HAL Id: hal-03475362

<https://hal.science/hal-03475362>

Submitted on 17 Feb 2023

HAL is a multi-disciplinary open access archive for the deposit and dissemination of scientific research documents, whether they are published or not. The documents may come from teaching and research institutions in France or abroad, or from public or private research centers.

L'archive ouverte pluridisciplinaire **HAL**, est destinée au dépôt et à la diffusion de documents scientifiques de niveau recherche, publiés ou non, émanant des établissements d'enseignement et de recherche français ou étrangers, des laboratoires publics ou privés.

Development of an in-situ measurement device for airfield pavement interface characterization¹

Maïssa Gharbi,² Michaël Broutin,³ Jean-Marie Roussel,⁴ and Armelle Chabot⁵

ABSTRACT

Regular pavement condition evaluation is the key to ensuring a good asset management of in-service pavements, for it allows anticipating and optimizing maintenance or rehabilitation works.

In particular, interface bonding conditions between asphalt concrete layers are of major concern since in most cases structural problems come from interface defects, and they furthermore have a huge impact on the pavement current mechanical behavior and its remaining service life.

Usual structural non destructive testing (NDT) devices do not allow assessing this parameter on their own. This is the reason why there is a need for an in-situ measurement system. The French Civil Aviation Technical Center (STAC) launched then an ambitious research and development program with the objective of developing a proof-of-concept for such a device and associated data analysis methodology, which enables characterizing the interface response for several mechanical solicitations including rolling-wheel passage or Heavy Weight Deflectometer (HWD) dynamic impulse load, with a twofold purpose: better understand for research purposes the interfaces mechanical behavior and its evolution during the life of the pavement; and have at disposal an operational tool to evaluate interface bonding condition of in-service pavements. This paper presents the measurement device developed by the STAC. It is inspired from the ovalization system invented in the 70's by the LPC (les Laboratoires des Ponts et Chaussées), which consists in measuring the diameter variation of a core-hole in three horizontal directions (longitudinal (L), transverse (T) and 45°) during the passage of a rolling-wheel. The first part of the paper focuses on the device development process which led to the final prototype. The second part is dedicated to the 3D-finite element modeling developed for data analysis. The results from a field survey, performed on the STAC's test facility, are finally presented and compared with numerical simulations.

¹M. Gharbi, M. Broutin, J.-M. Roussel, and A. Chabot, "Development of an In Situ Measurement Device for Airfield Pavement Interface Characterization," *Journal of Testing and Evaluation* 50, no. 2 (March/April 2022): 818–835. <https://doi.org/10.1520/JTE20210211>.

²French Civil Aviation Technical Center (STAC), F-94385 Bonneuil-s-Marne, France ; <https://orcid.org/0000-0002-5720-9943>

³French Civil Aviation Technical Center (STAC), F-94385 Bonneuil-s-Marne, France ; <https://orcid.org/0000-0002-8446-8019> - corresponding author : michael.broutin@aviation-civile.gouv.fr

⁴French Civil Aviation Technical Center (STAC), F-94385 Bonneuil-s-Marne, France ; <https://orcid.org/0000-0002-4392-6095>

⁵Univ Gustave Eiffel, MAST-LAMES, F-44344 Bouguenais, France ; <https://orcid.org/0000-0002-9430-8457>

Keywords

Airfield pavement, interface characterization, in-situ assessment, ovalization, HWD, 3D-Finite Element modeling.

Introduction

Regular pavement condition evaluation is the key to ensuring good asset management of in-service pavements, for it allows anticipating and optimizing maintenance or rehabilitation works. In particular, interface bonding conditions are of major concern because in most cases structural problems come from interface defects, and furthermore, they have a huge impact on the pavement current mechanical behavior and its remaining service life. It actually significantly affects the stresses and strains observed in the asphalt course, as it is numerically demonstrated in Roussel et al.¹

The phenomenon of asphalt slippage cracking is a serious concern, especially for airfield pavements. Indeed, several cases of debonding between layers and slippage in hot-mix asphalt layers have been observed at different airports in the last few years. The slippage failures occur especially at high temperature on runways at the high-speed taxiway exit when airplanes brake and turn. For example, a number of transversal cracks have been observed, during the summer months, at the airfield pavement surface in the Australian Melbourne Airport runway, especially at the heavy braking and turning zones.² Newark International Airport Runway 4R-22L in New Jersey (USA) had experienced slippage at the interface of the two first asphalt layers in the heavy breaking/turning areas of the high-speed taxiway.³

In fact, even if it has been demonstrated⁴ that it is possible to detect (large enough) interface defects from measured deflections, it is complex in practice to identify during the data analysis phase a specific signature for interface defects because lower asphalt moduli would have the same effect on the deflections. Figures 1 and 2 highlight that usual structural NDT devices such as the heavy weight deflectometer (HWD) are not sufficient on their own to assess the interfaces condition.

Figure 1 presents results from an HWD test campaign performed in 2012–2013 on the circular Accelerated Pavement Testing (APT) facility of Université Gustave Eiffel in Nantes, France, on the structure containing 3 by 1.5 m artificial defects (sand at interface, geotextile, lack of tack coat). A backcalculation process based on a dynamic 3-D Finite Element (FE) modeling was performed using the deflections obtained in the bonded interfaces area and forward calculations with fully sliding interfaces using the backcalculated moduli set enabled to find the deflection levels obtained in the defects area (fig.

1A).⁴ The deflection basins obtained by extracting peak values for each deflection time-history (fig. 1B) present the same trend as those obtained by taking into account an interface stiffness parameter such as that developed by Roussel et al.¹

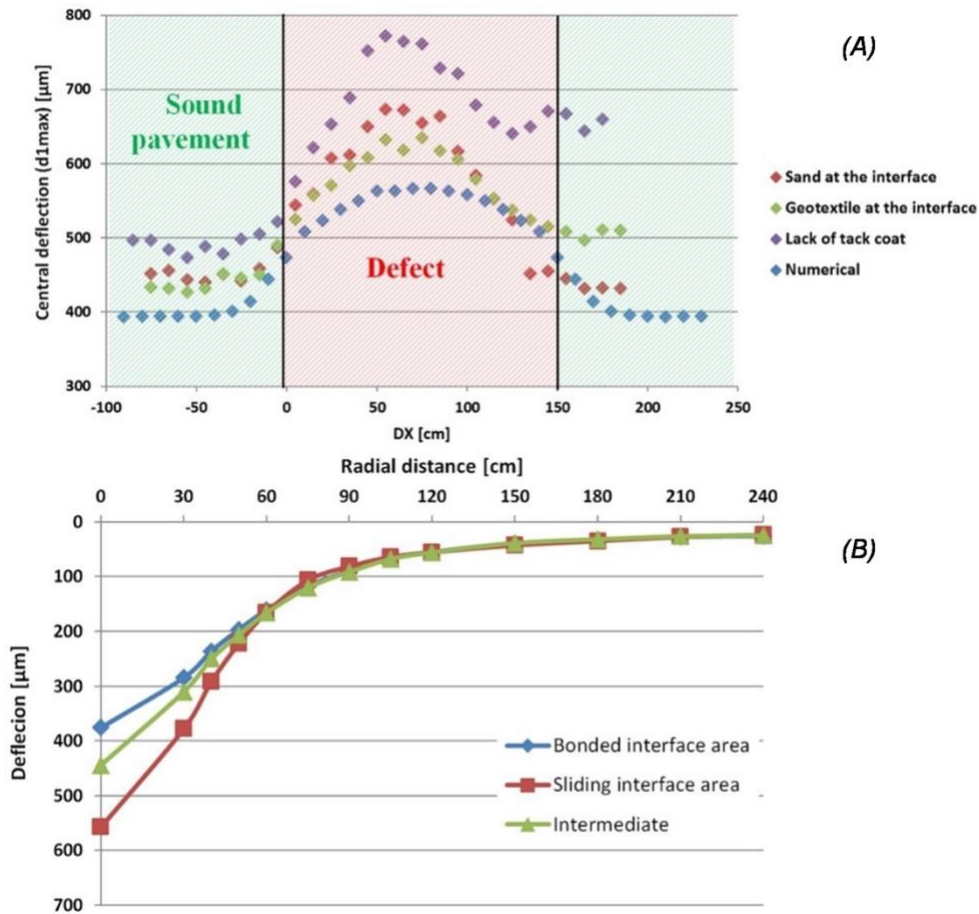


FIG. 1 Influence of interface defect on HWD deflections, in situ results (A) central peak deflection (from Sadoun, Broutin, and Simonin⁴) and (B) selected deflection basins.

Figure 2 presents selected raw results from a 1-year experiment conducted on the STAC’s test facility⁵ at Bonneuil-sur-Marne in France, with the objective of studying the influence of temperature in the (sound) bituminous materials on deflections and improving temperature correction law on backcalculated moduli.⁶ Observed extreme values for the mean asphalt concrete layer temperature were 0°C and 30°C.

Crossing the results from these two experiments makes it then possible to confirm there is no specific signature of an interface defect when studying surface deflection, and it is complex to distinguish it from a decrease in asphalt concrete moduli because of the following:

- In both cases, central deflections increase, and outer deflections are not impacted,
- Significant discrepancies can be observed on central deflections for both asphalt moduli variations

(due to damage) or interface conditions, and all intermediate cases are possible combining partially bonded interface and undefined material residual properties between sound material and material reaching the failure (moduli divided by two).

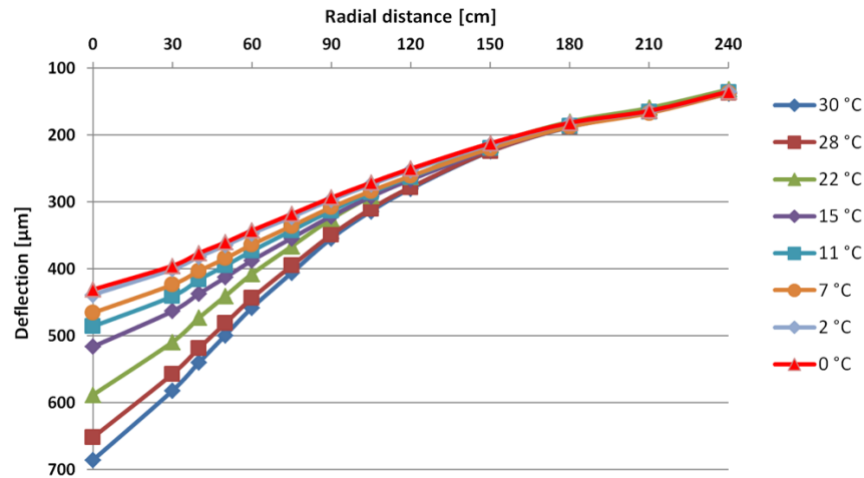


FIG. 2 Influence of asphalt layer moduli variation (due to temperature effect in this instance) on HWD surface deflections.

This is the reason why there is a need for an in situ measurement system, to be combined with HWD tests, for a reliable assessment of both materials residual properties and interface conditions simultaneously. Besides, the necessity of developing in situ measuring devices to detect and evaluate interfaces defects was highlighted by the RILEM Mechanisms of Cracking and Debonding in Asphalt and Composite Pavements technical committee (TC241-MCD) in its final recommendations⁷ and State-of-the-Art report.⁸

In that objective, the French Civil Aviation Technical Center (STAC) launched an ambitious research and development program with the objective of developing a proof-of-concept for such a device and associated data analysis methodology, for use in the case of airfield pavement. This device would enable measurements under both rolling-wheel loads or HWD dynamic impulse loads applied on a stationary loading plate.

The main purposes of this study are to better understand interfaces mechanical behavior and evolution for research purposes and to have at our disposal an operational tool to evaluate the interface bonding condition of in-service airfield pavements. The first part of the paper focuses on the device development process that led to the final prototype. The second part is dedicated to the 3-D finite element modeling developed for data analysis. The results from a field survey, performed on the STAC test facility,⁵ are finally presented and compared with numerical simulations.

Materials and Methods

PROOF-OF-CONCEPT FOR AN IN SITU MEASUREMENT SYSTEM

Previous Developments of Ovalization Devices

Based on the equations of mechanical fields concentrated around holes,⁹ the measurement device developed by the STAC presented in this paper is inspired from the ovalization system which was developed in the 1970s by Kobisch, and Peyronne,¹⁰ from the LPC (les Laboratoires des Ponts et Chaussées). This device aims to evaluate in situ interface bonding conditions between road pavement layers and to approximate the strains inside the multilayered structure due to a surface loading, which consists of measuring the diameter variation of a core-hole in three horizontal directions (longitudinal [L], transverse [T], and 45°) during the slow passage of a rolling-wheel (fig. 3).

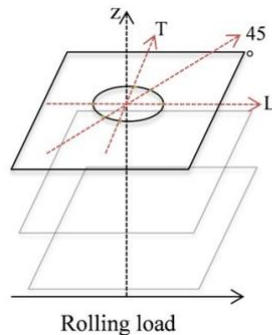


FIG. 3 The three-plane direction (from Gharbi et al.¹¹).

Main Findings from the Evaluation of the Current Version

The current version of the device proposed by Ruiz and Voisin¹² derives from successive evolutions of the system between 1974 and today,^{13,14} described by Gharbi et al.¹¹ It was evaluated for airfield pavement.¹⁵ A test campaign was conducted in 2018 in partnership with the CEREMA (Centre d'études et d'expertise sur les risques, l'environnement, la mobilité et l'aménagement) at the STAC's full-scale airfield pavement test facility constructed on the Centre d'Expérimentations Routières (CER) site (Rouen, France).¹⁶ For slow-rolling loading conditions,¹⁶ the conventional tests showed satisfactory results. By contrast, measurements obtained under HWD impulse load presented some limitations:

- An oscillation shape is observed for all measured signals, which derives from mechanical vibrations of the probe,
- The data acquisition rate (130 Hz) which is the maximal rate applicable for this device is insufficient to obtain exploitable measurements,
- The current system does not enable performing diameter measurements at the pavement surface,

neither carrying out HWD tests with the load plate centered right above the core-hole (axisymmetric configuration).

The conclusions from this experiment confirm the need to develop a dedicated device for airfield needs or measurements involving HWD load tests, in order to overcome the aforementioned limitations. The technical requirements for this device are detailed hereafter. Furthermore, the analysis method needs to be modernized.

Expected Technical Specifications for In Situ Measurement System

First, the system needs to enable core-hole deformation measurements under several solicitation types such as static heavy loads, rolling-wheel airfield loads or HWD dynamic impulse loads, involving a loading plate positioned at different distances from the core-hole, including a centered position above it, which implies the following:

- At least a 300-Hz acquisition rate and preferably 1 kHz. Indeed, the HWD load signal pulse time is approximately 30 ms, which makes it representative of an aircraft rolling-wheel on runway (300 km.h⁻¹)¹⁷; a minimum of 10 records within this timeframe is required to reconstitute properly load and deflection signal shapes; in practice, the input force signal presents generally a double peak, meaning that higher frequencies are recommended,
- A mechanical system stable enough in order to avoid any parasitic vibrations,
- Preferably a wireless acquisition system.

Simultaneous multidepths measurements are also required, at four depth levels within the bituminous course, including measurement near pavement surface level: surface level, above and below the interface between surface and base course, and bottom of the base course. Finally, a particular attention will be paid to propose an easy setting up of the device in the core-hole.

Full-Scale Validation Tool

A full-scale airfield pavement test facility was constructed by the STAC5 on its site (Bonneuil-sur-Marne, France) to validate flexible airfield pavement mechanical models and study NDT devices or technical innovations, among others. The flexible pavement is a conventional airfield flexible pavement composed of a French standard bituminous material (NF EN 13108-1, Mélanges bitumineux-Spécifications des matériaux - Partie 1 : enrobés bitumineux) called BBA (0/14 class 3) for the surface layer ($E = 10,500$ MPa at 15°C and 10 Hz; $\nu = 0.35$), a standard French bituminous material called GB (0/14 class 3) for the base layer ($E = 15,600$ MPa at 15°C and 10 Hz; $\nu = 0.35$), and a standard French UGA layer, named GNT (0/31.5 type B), for the subbase layer, placed upon a 50-MPa bearing capacity

(PF2) subgrade. The pavement structure presents, in theory, fully bonded interfaces because a tack coat emulsion was applied at construction stage, and this pavement is not trafficked.

The test facility was specifically equipped in 2019 in the frame of this research project with three 162-mm-diameter core-holes and three 300-mm-diameter ones. The cores were retained and equipped with lifting eyes, which enables removing them for test campaigns and repositioned in the core-hole after tests using a sealing system in order to avoid any water infiltration within the pavement foundation. The prototype proposed in this paper is adapted to 162-mm-diameter core-holes.

The layer thicknesses are well known from several ground penetrated radar (GPR) surveys combined with corings; their values in the area of the aforementioned core-holes are given in the following section. Approximate layer elastic moduli values are available, thanks to several HWD test campaigns, such as a 1-year long experiment

involving weekly tests,⁶ which demonstrated from dynamic back-calculations that the subgrade and GNT layer moduli remain stable during a whole year, around 184 MPa and 250 MPa, respectively, and also to laboratory complex moduli performed on extracted BBA and GB samples: these types of tests were performed after construction in 2007, and new tests performed in 2019 showed that the material properties were nearly unchanged.

STAC's Prototypes

General Prototype Concept and Variants

It is decided in the frame of this proof-of-concept phase to develop a one-level self-supporting system, which could in a next step be duplicated and easily integrated into a multilevel measurement system.

Two variants of such a prototype were developed and presented in earlier versions in Gharbi et al.¹⁵ and evaluated in situ. Their design is based on a common concept of a self-bearing horizontal tray equipped with displacement sensors positioned in pairs for each plane direction (L, T, 45°) (fig. 3). The selected sensors are the 2 screws strain sensors DD1 (displacement transducers measuring displacement and strain with an accuracy class of 0.1), developed by HBM Test and Measurement Company. They are so characterized by a measurement range of ± 2.5 mm and an uncertainty below 0.5 %. The measurement principle relies on the bending measurement of a steel blade. A QuantumX data acquisition unit (from HBM Test and Measurement) is used, which permits attaining the required 4,800-Hz acquisition frequency per measurement channel. The mechanical systems were designed using the SolidWorks CAD software, and the prototypes presented here were manufactured in plastic with a 3-D printer. It should be noted that all prototypes were designed for 162-

mm-diameter core-hole, but their design could easily be adapted for measurements within core-holes of other diameters.

First Variant

The first variant of the prototype is composed of two overlapping trays (fig. 4).

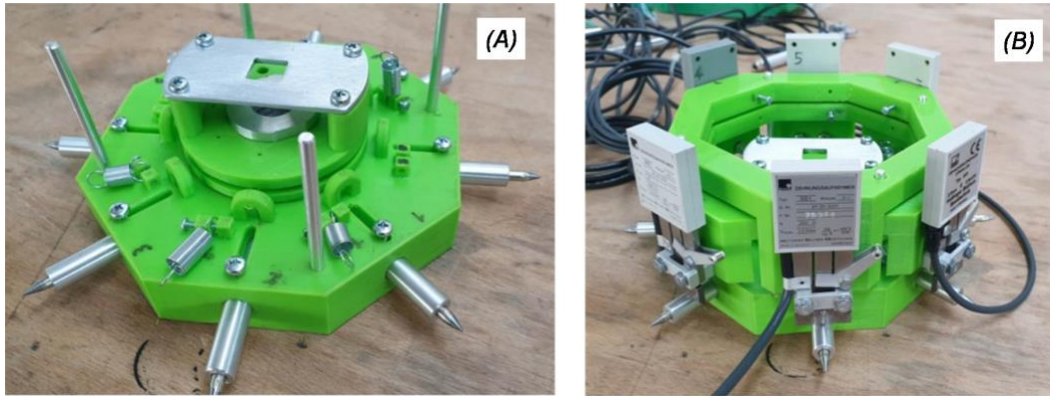


FIG. 4 First variant of the prototype: (A) isolated view of the lower tray; (B) assembled system.

The lower one ensures the holding of the device in the core-hole at the selected depth by means of eight metal tips pressing on the inner cavity wall with individual compression springs (fig. 4A). The metal tips can be easily folded up for dismounting or released for positioning in the core-hole through an automated system composed of a nylon thread and a central screw. The upper part, positioned in a second step and screwed on the lower one, maintains the sensors (fig. 4B).

Second Variant

The second variant of the prototype consists of a unique self-bearing tray (fig. 5). Details of its SolidWorks mechanical drawings are given in the Appendix (fig. A.1).

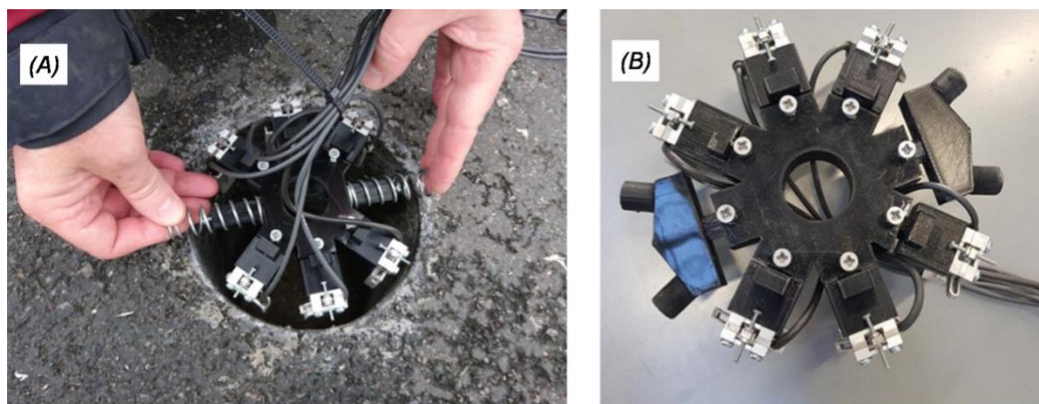


FIG. 5 Second variant of the prototype: (A) early version (spring fixing system); (B) final version (telescopic system with buffers).

The eight metal tips and springs are replaced by a fixing system in the unused 45° plane direction. This

fixing system comprised in the early version of this prototype in two stiff springs (fig. 5A), which were replaced in the upgraded versions by a telescopic system equipped with rubbers and to which a pretension is applied through a vertical screw (fig. 5B).

Dedicated Laboratory Validation Bench

A dedicated laboratory validation bench was developed to verify the measurements provided in a hollow cylinder by the final prototype. It consists of a 162-mm-diameter hollow plastic cylinder, manufactured by means of a 3-D printer. The cylinder is mounted on a circular support equipped with attachment systems for six reference LVDT (Linear Variable Differential Transformer) displacement sensors (fig. 6). The DD1 sensors of the prototype and the LVDT (Linear Variable Differential Transformer) are aligned through the plastic, and their respective measurements are compared when applying deformations to the cylinder.

Prototype Development Process

A two-step development process was followed: a preliminary feasibility study to validate a final prototype and a final field validation involving this selected prototype to be used for comparisons between field and numerical results.

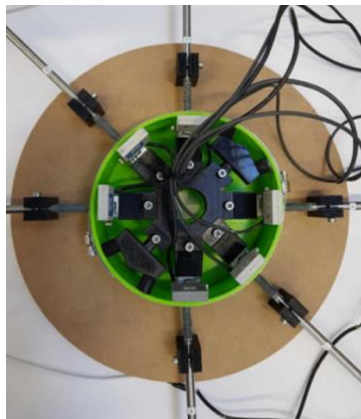


FIG. 6 Dedicated verification and calibration bench: experimental system.

Preliminary Feasibility Study

The preliminary validation phase of the prototype focused specifically on the following aspects:

- the mechanical stability, which means the device should not move in the core-hole during the tests, and no parasitic vibration should be observed on measurements,
- an easy and quick set-up, and
- a good measurement repeatability.

For this in situ validation phase made on the STAC full-scale airfield pavement structure (fig. 7A), it was

decided to use HWD tests involving high load levels and especially to position the HWD load plate adjacent to the core-hole (fig. 7B). The dynamic impulse load provided by this device is more constraining with respect to the mechanical stability issue than static or rolling-wheel loads. Tests were conducted in 2019 under HWD impulse loading. Three HWD load levels are applied, corresponding to the respective $F1 \sim 260$ kN, $F2 \sim 170$ kN, and $F3 \sim 130$ kN peak values, and for each load level, 5 drops are performed for repeatability study, with an acquisition rate of 4,800 Hz.

General Test Plan for Final Field Validation

A test campaign was carried out in July 2020 on the STAC's test facility which involved:

- HWD tests at several distances (d_i) from the core-hole: $d1 = 0$ cm, i.e., HWD load plate centered over the core-hole; $d2 = 22.5$ cm, i.e., load plate adjacent to core-hole; and $d3 = 52.5$ cm and $d4 = 82.5$ cm, i.e., distances between plate and core-hole edges of 30 and 60 cm, respectively. For each test, two load levels were applied to study the linearity of the response, and for each of them, three drops were performed to evaluate repeatability; the regular HWD setting for airfield pavement was respected, i.e., a 45-cm segmented plate was used; a 4,800-Hz acquisition rate was selected, and a dedicated connection was implemented in order to duplicate the HWD load signal measurement and record it simultaneously, on the same data acquisition unit, with the prototype displacement sensors, which enables ensuring synchronized measurements;
- the final prototype positioned successively at each of the four measurement levels defined here previously, i.e., pavement surface, above the BBA/GB interface, below the BBA/GB interface and at the bottom of the GB layer, in one of the 162-mm-diameter core-hole.

It is decided to focus in this paper on the centered position, for the highest load level (~ 190 kN). This position presents the advantage of proposing an indirect field validation of the prototype, because the measurements in the three plane directions should be equal due to axisymmetric configuration. The mean temperatures within the BBA and GB layers during the test sequence were, respectively, 40.5°C and 33.1°C . The evaluation of the corresponding moduli at those respective temperatures and for a 30-Hz frequency (corresponding to the pseudofrequency of the HWD load signal pulse time) from the 2019 complex moduli tests, are, respectively, 800 and 5,700 MPa. For the record (see previous), subgrade and foundation layer elastic moduli have been determined from previous HWD test campaigns and dynamic backcalculation process. The obtained values are, respectively, 250 and 184 MPa. Table 1 summarizes all values, which will be retained in the next session.

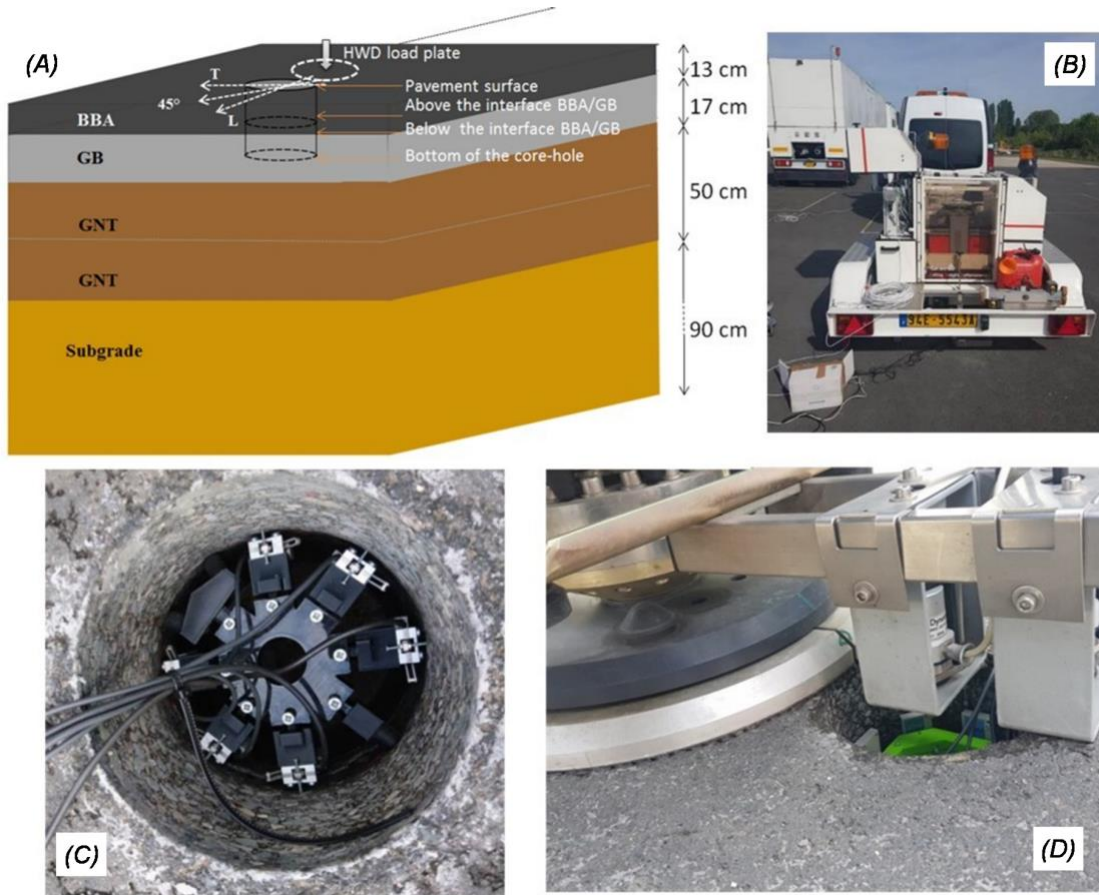


FIG. 7 Field validation: (A) STAC’s test facility and test configuration (after Gharbi et al.15); (B) HWD on the test area; (C) prototype (second variant) in a core-hole; (D) HWD test with load plate adjacent to the core-hole.

TABLE 1 Synthesis of pavement layer moduli

| Layer | Surface asphalt concrete (BBA) | Base asphalt concrete (GB) | UGA (GNT) foundation layer | Subgrade |
|--------------|--------------------------------|----------------------------|----------------------------|----------|
| Moduli [MPa] | 800* | 5,700* | 250 | 184 |

*Norm of complex moduli at 30 Hz

DEDICATED NUMERICAL ANALYSIS TOOL

A 3-D finite element model was developed for data analysis, using COMSOL Multiphysics software. The mesh includes the HWD load plate and the core-hole (fig. 8). It contains a symmetry plane, which passes through the core-hole and load plate centers. A Dirichlet condition is retained for boundary conditions, which imposes a normal displacement null for all mesh boundaries. A script was developed to automate the mesh creation as a function of the pavement layers thicknesses and load plate position from the core-hole.

Modeling

Resolution Method

A linear elastic dynamic time-domain modeling is proposed so far, which is similar to that described in the French Technical Guidance for Flexible Airfield Pavement Assessment Using HWD,¹⁷ for axisymmetric problems. In this approach, inertia effects are taken into account through the classical discretized equation (1):

$$M \ddot{u}(t) + K u(t) = P(t) \quad (1)$$

with M and K , respectively, the mass and stiffness matrices, $u(t)$ the displacement vector at t time, and $P(t)$ the vector containing external strengths.

The HWD force signal is used as an input mechanical solicitation. It is approximated by a linear interpolation.

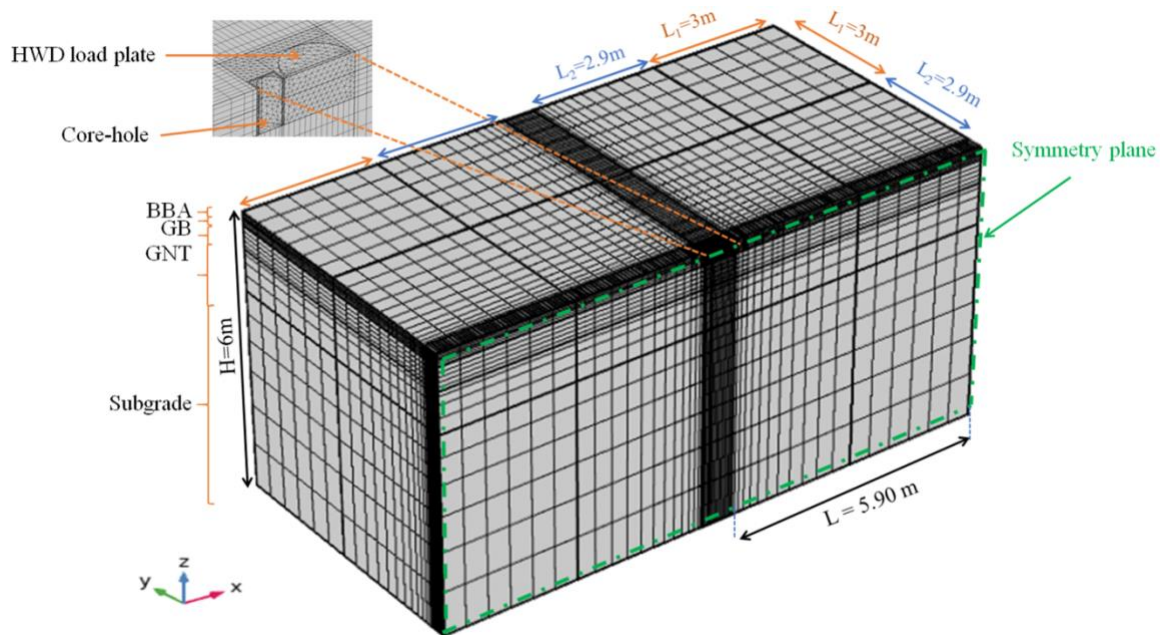


FIG. 8 FE mesh, 3-D view (after Gharbi et al.¹⁵).

Interface Modeling

Two interface behaviors were implemented so far: fully bonded interfaces or fully sliding ones. Two approaches were studied and compared for fully sliding interfaces: on one side, double-nodes with an equality condition on vertical displacements and no constraint on horizontal components. On the other hand, the introduction of an anisotropic thin layer without thickness presenting a high modulus in the vertical direction and a very small moduli in the horizontal directions. Calculations performed for both approaches provide the same results. It should be noted that the second approach could be used in the

future to implement, if needed, partially bonded interface conditions in the modeling, by adequately selecting the horizontal moduli values.

Mesh Optimization

The default mesh height is 6 m. It was demonstrated¹⁸ that this height is sufficient to simulate semi-infinite subgrade for dynamic simulations. This height can be reduced to consider shallow bedrocks, which is not the case for the STAC’s test facility. The mesh lateral extension and the element sizes were optimized in order to avoid, respectively, any undesirable wave reflections on the mesh lateral boundaries and optimize computation times. The mesh includes (fig. 9) a fixed part outside the “core-hole and load plate area” according to the X-axis, and a central strip of Δ width, with Δ the distance between the core-hole and load plate edges (which implies that the total length of the mesh is not constant and depends on the load plate position from the core-hole). Within the “core-hole and load plate area” (fig. 9B), it is composed of tetrahedral elements near the surface and prismatic elements below and of parallelepiped for the rest of the mesh. These are order 2 Lagrange elements with a quadratic interpolation.

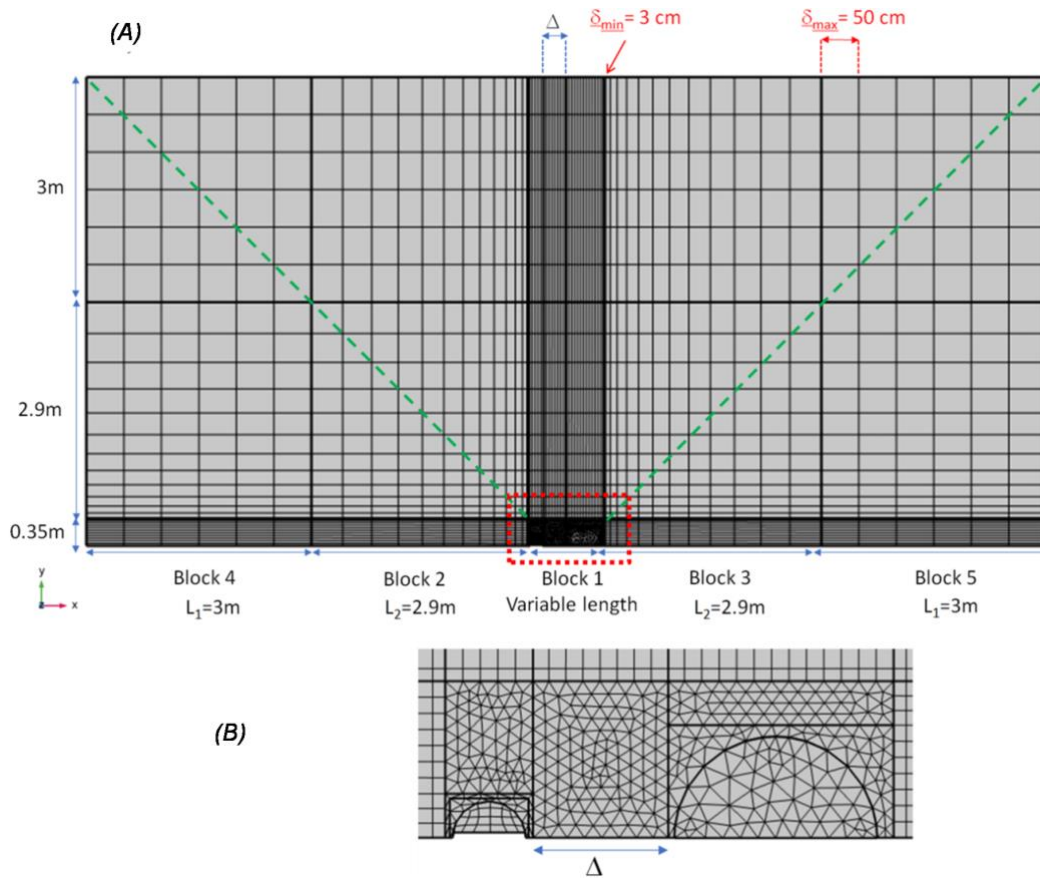


FIG. 9 FE mesh, XY top view: (A) general overview; (B) zoom on core-hole and load plate area (framed with red rectangle shape in general overview).

A geometric distribution is chosen for the elements size in Blocks 2 and 3 for the X-direction, with a smaller element of δ_{\min} size and, and a larger one of δ_{\max} size (fig. 9A), and a constant δ_{\max} size for outside Blocks 4 and 5. The same elements sizes are retained for the Y-direction (see the symmetry with respect to the green diagonal dotted lines on fig. 9A). A constant δ_{\min} size is chosen for the Block 1 parallelepiped elements outside the “core-hole and load plate area.” Finally, the tetrahedral and prismatic elements in the “core-hole and load plate area” are automatically generated by ComSol on the basis of this δ_{\min} discretization on its outer edge.

The optimization process consists then in determining the δ_{\min} and δ_{\max} values, and the distance between load plate or core-hole edges to the mesh boundaries, i.e., the $L = L1 + L2$ length, which corresponds to the summation of the Block 2 and Block 4 widths (fig 9A). The precision criteria retained are 1 μm for the diameter variation and HWD deflections, 1 $\mu\text{m}/\text{m}$ for strains, and 0.1 MPa for stresses. The results led to retain the respective 3 cm and 50 cm values for δ_{\min} and δ_{\max} , and it was demonstrated that a 6-m distance between load plate or core-hole center and mesh boundary is sufficient, which is respected in the figure 9 mesh. This leads to a 20,000 elements mesh for the configuration where the load plate is adjacent to the core-hole.

Note that this optimization work was performed for standard moduli at (20°C, 30 Hz) for bituminous materials, i.e., respectively, 9,000 MPa and 13,900 MPa for the BBA and GB layers and for a fully bonded interface. It is assumed that these results remain valid for other moduli set and interface conditions.

Results and Discussion

IN SITU AND LABORATORY DEVICE VALIDATION

Learnings from Feasibility Study

The setting up of both STAC prototype variants in the core-hole turned out to be simple and quick to perform. It is suggested to use the existing core-holes performed to calibrate GPR in the frame of layer thicknesses determination. Actually, changing the prototype depth within the core-hole requires approximately 5 minutes, and it implies moving and repositioning the HWD, which requires an extra 2 minutes. A 30-minute timeframe is then sufficient to test all four depths. Nevertheless, an oscillation shape is observed for all measurements provided by the first variant as illustrated in figure 10A, which is attributed to parasitic mechanical vibrations. This phenomenon was already noticed for early measurements at the surface.¹⁷ These oscillations may be related to the spring system. Attempts to

improve the prototype, such as modifying the springs stiffness, did not solve the problem. On the contrary, measurements performed with the second variant present a regular shape (fig. 10B) for all depths and in all the three (L, T, 45°) directions. Furthermore, the compact design of the second variant is an advantage for the next prototype development step, which will consist of upgrading the system for simultaneous multilevel measurements. It is then decided to retain the second variant in its final version for future works (fig. 5B).

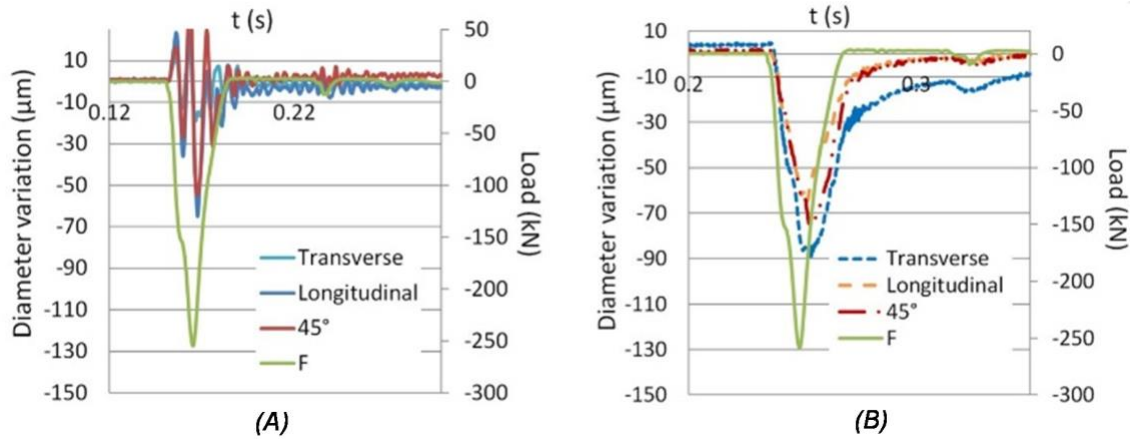


FIG. 10 Examples of core-hole diameter variation time-histories measured above the BBA/GB interface during the 2019 feasibility tests (HWD load plate adjacent to core-hole, $F_{max} \sim 260$ kN, mean temperature in bituminous layer $\sim 35^\circ\text{C}$): (A) first variant; (B) second variant.

Learnings from Laboratory Tests

The final prototype was evaluated using the laboratory test bench (fig. 11). Positive results were obtained (fig. 11A), which confirms the diameter variation measured by the prototypes is reliable.

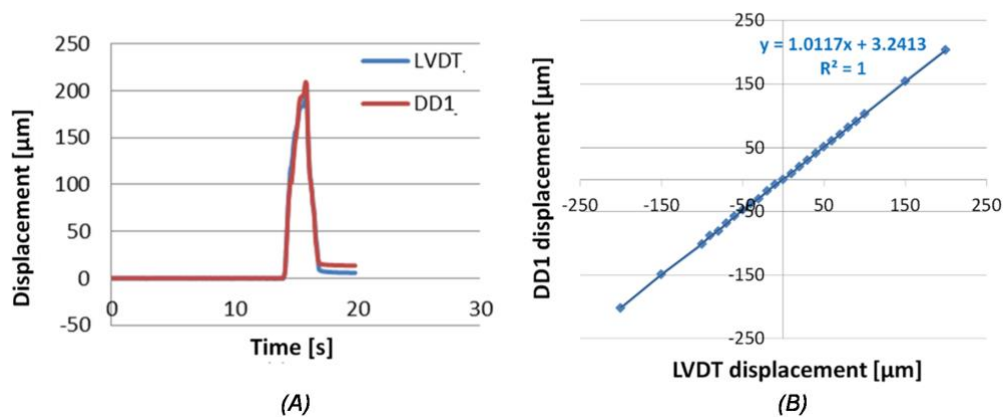


FIG. 11 Dedicated verification and calibration bench: (A) example of comparison between DD1 and LVDT (Linear Variable Differential Transformer) time-histories; (B) example of calibration results.

The system was also used as a calibration bench for the prototype (fig. 11B), using the same experimental protocol. It should be mentioned that this calibration bench is a proof-of-concept itself; work is in progress to adapt a similar system on a precision electromechanical laboratory press with a metal cylinder placed between two thick metal plates.

Learnings from Final Field Validation

The comparison between field and numerical results constitutes an indirect validation of the prototype measurements. Actually, the field results are coherent with theoretical expectations. Furthermore, similar core-hole deformations are measured in the three plane directions, which was expected due to the problem axisymmetry.

Those observations will be detailed in the next section.

COMPARISON BETWEEN NUMERICAL AND FIELD RESULTS

Analysis of Core-Hole Diameter Variation Envelope Profile

The peak values extracted from either experimental data or dynamic simulation results, respectively, for fully bonded and fully sliding BBA/GB interface are presented for the three plane directions in Table 2, as well as the related mean values and standard deviations.

TABLE 2 Comparison between field diameter variations and FEM simulations results

| | Field results [μm] | | FEM simulations [μm] | |
|------------------------|--------------------|---------------------|------------------------|-------------------------|
| | Mean values | Standard deviations | Fully-bonded interface | Fully-sliding interface |
| Pavement surface | -175.3 | 15.9 | -203.7 | -108.4 |
| Above BBA/GB interface | -73.8 | 0.9 | -55.5 | 93.0 |
| Below BBA/GB interface | -74.4 | 37.2 | -49.6 | -86.6 |
| Bottom of GB layer | 75.4 | 12.1 | 41.8 | 50.6 |

Because of the aforementioned quick setting up of the prototype in the core-hole, it is decided to ignore the temperature variation within the bituminous course during a test sequence. It is then possible to reconstitute a core-hole deformation profiles as if all four tests were performed simultaneously, provided that the target load is unchanged between tests and the tests are repeatable. Note that the following sign convention is maintained: a core-hole positive diameter variation (“opening”) is presented as positive, whereas a core-hole negative diameter variation (“contraction”) is presented as negative.

Similar core-hole deformations are observed in the three directions. This result is as expected, the

mechanical problem being axisymmetric for the retained HWD load plate position. The mean experimental envelope corehole profile and associated standard error bars are presented in figure 12, as well as the theoretical profiles for both fully bonded interfaces and fully sliding interfaces numerical simulations.

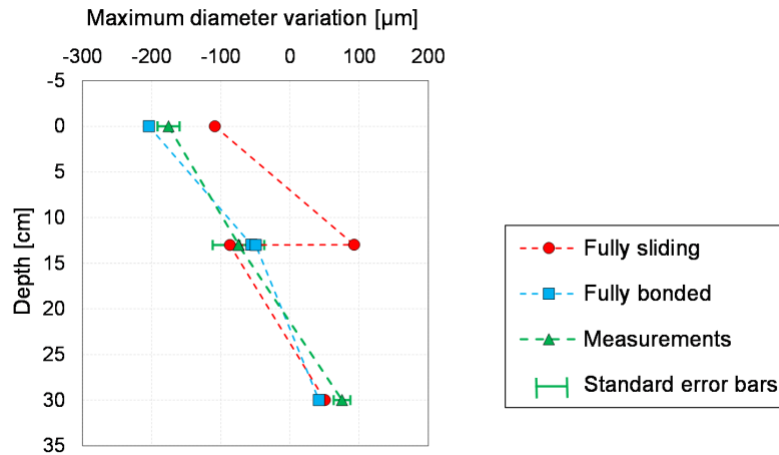


FIG. 12 In situ measured envelope diameter core-hole variation profile and associated error bars versus FEM simulations for fully bonded and fully sliding interfaces.

It should be stressed that a higher standard deviation is obtained for the measurement level below the BBA/GB interface. It is linked to an abnormally high longitudinal core-hole deformation compared with the transverse and 45° deformations, which give similar results, as illustrated in the following figure 13C. This measurement is considered as aberrant.

First, the results tend to confirm that the measurement system is adapted to the problem. In fact, the standard error bars are small enough compared with the observed displacement differences between the fully bonded and fully sliding simulations for the device to provide discriminatory information about interface condition.

Secondly, the analysis of the results obtained at the different levels points out the following:

- The observed surface measurements are comprised between fully bonded and fully sliding simulations, but very close to the fully bonded results;
- The measurements above and below the interface are very close, the discrepancies between respective mean values being very small compared with the uncertainties mentioned previously, which also suggests that the interface seems to be bonded;
- The measurements above and below the interface are close to numerical expectations for fully bonded

interface (contraction, the interface being here above the neutral axis for which radial strain and core-hole diameter variation are null, whereas a sliding interface would have led to an opening of the surface layer at his base); and

- consistent results are observed between field results and numerical simulations at the base of the base layer; note that the diameter variation at this depth is not discriminatory for interface evaluation, the numerical simulation providing similar results for this parameter.

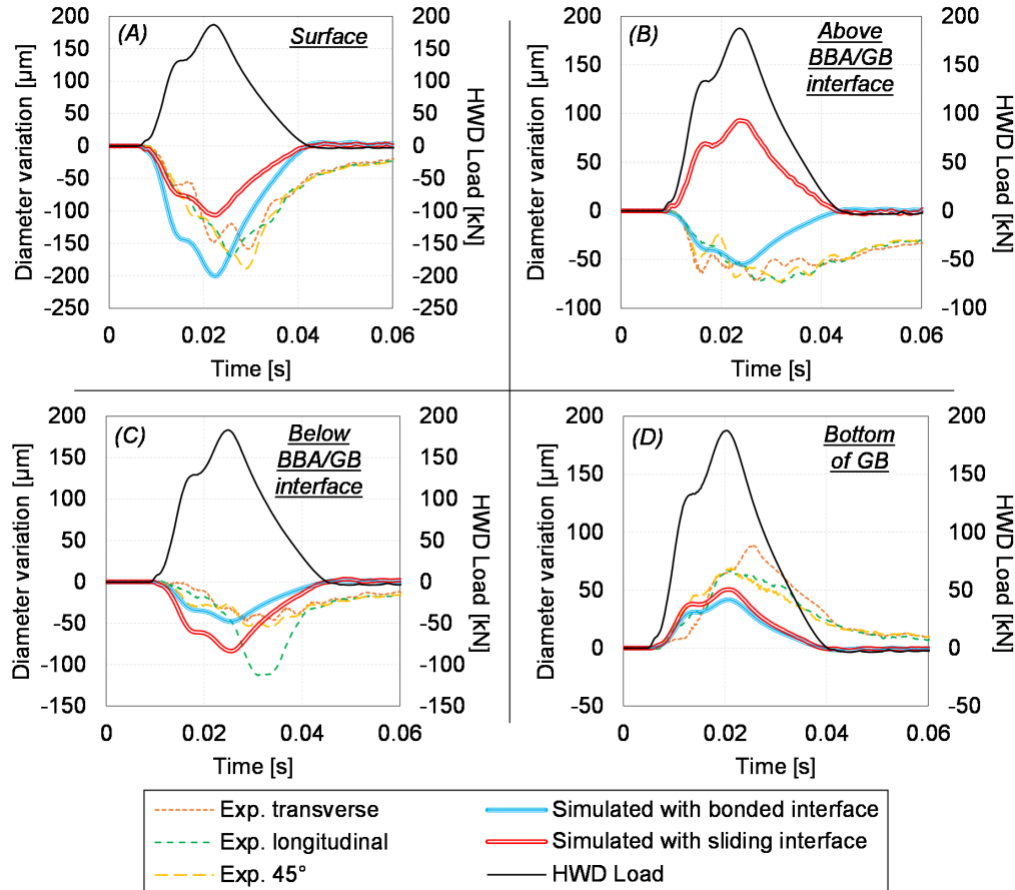


FIG. 13 In situ core-hole diameter variations time-histories (HWD test case with load plate centered above the core-hole) versus FEM simulations for fully bonded and fully sliding interfaces: (A) at the surface level; (B) above the BBA/GB interface; (C) below the BBA/GB interface; and (D) at the bottom of the GB layer.

It should be noted that the numerical results are affected by the selected moduli set. These moduli were as aforementioned obtained from backcalculation for subgrade and foundation layers, considering a fully bonded BBA/GB interface,⁴ and from laboratory complex moduli tests for asphalt concrete materials. One of the next challenges could be to refine the evaluation process by combining HWD data and core-hole diameter variation measurements in a global backcalculation process on both moduli and interface condition. This point will be expanded hereafter.

Analysis of Core-Hole Diameter Variation Time-Histories

The experimental and numerical diameter variation time-histories for the four depths are presented in figure 13.

It can be noticed that a time-delay is observed for the experimental peaks against the numerical results and the descending parts of the experimental signals, after the peak, present a slower return to zero than the numerical curves.

These observations may be explained by viscous effects, not taking into account in the considered elastic modeling. Viscoelastic behaviors for materials and interfaces modeling could be introduced in the future to confirm this hypothesis and refine the numerical approach.

Consistency of HWD Deflections

The figure 14 illustrates the numerical deflection basins for both fully bonded and fully sliding simulations and one of the four experimental basins, a good repeatability being observed between the four tests. The central deflection was not measured because the plate center was not in contact with the pavement due to the core-hole.

The general expected behavior described in the introduction of this paper is observed, i.e., discrepancies on deflections near the load between bonded and sliding simulations and the same outer deflections.

The experimental deflections are close to fully bonded simulation results, strengthening the previous results on the core-hole diameter variations and the consistency of the study, but lower deflections are obtained, which means the selected moduli set may be refined.

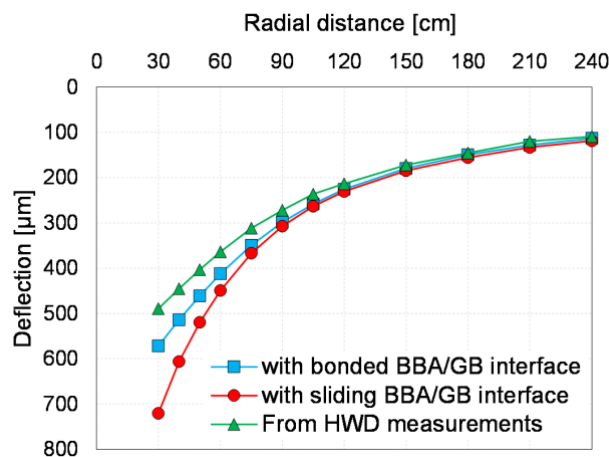


FIG. 14 Experimental HWD deflection basin versus FEM simulations for fully bonded and fully sliding interfaces.

Because there is, as explained in the introduction, a competition between interface conditions and

asphalt moduli variations, and no specific signature for interface defects, the only way to reliably determine all parameters would be to have a backcalculation process using as input data deflection and core-hole diameter variations. This would enable determining simultaneously material residual characteristics and interface conditions.

The next steps for this work could then be to first implement the partially bonded interface behavior in the elastic modeling, for example, using an interface stiffness and implement a dynamic backcalculation process on both surface deflection and core-hole diameter variation time-histories to determine the elastic moduli and interface stiffness. Viscoelastic behavior for materials and interfaces could be introduced in a second step if needed for backcalculations and forward calculation steps, the final objective being to evaluate, as reliably as possible, the interface condition from backcalculation process and a pavement remaining life from forward calculation, and if needed to design an overlay.

Conclusion

The need to develop field interface condition evaluation systems, in order to ensure an optimized airfield pavement asset management, was highlighted in this paper. This presents the first results from a recent STAC research and development program. A proof-of-concept for an in situ measurement device for the characterization of the airfield pavement interfaces between asphalt concrete layers as well as an associated analysis method are presented.

A prototype was developed which enables measuring the diameter variation of a core-hole at any depth within the bituminous layer, including the pavement surface and the bottom of the bituminous course under the influence of mechanical surface loading. This prototype was evaluated in terms of speed and easiness of operational setting up, mechanical stability under surface plate dynamic impulse loads and metrological reliability. Its design was thought in such a way that it would be easily upgraded to a multilevel measurement system. The next prototype evolution should propose the possibility to simultaneously measure a core-hole diameter variation at four depths, which could be classically the surface level, above and below the surface/base asphalt concrete interface, and at the bottom of the base asphalt concrete layer. Other middle-term developments are expected such as the use of noncontact sensors or a wireless data acquisition system.

A 3-D dynamic finite element modeling was developed, which enables calculating, at any depth, the core-hole diameter variations time-histories implied by HWD surface dynamic impulse loads. Fully bonded or fully sliding interface behaviors were implemented as of now, but partially bonded conditions

could be introduced. A full-scale validation was performed on the STAC's instrumented test facility, which presents, in theory, fully bonded interfaces because a tack coat emulsion was applied at construction stage, and this pavement is not trafficked. This validation involved HWD tests with the load plate centered above the core-hole or positioned at several distances from it. The comparison, for the load plate-centered position, between experimental and numerical core-hole diameter variation envelope profiles and time-histories for the four studied levels (surface, above and below the interface, bottom of the bituminous course) demonstrated that the field results were very close to the numerical results for the fully bonded interface condition and that viscous effects were highlighted. Viscoelastic behaviors for materials properties and interface could then be implemented in the modeling. The complementarity between the HWD surface deflection measurements and core-hole deformation was also pointed out in order to evaluate both material residual properties and interface conditions. It was also brought out that the analysis of those deflections or core-hole diameter variation measurements separately was not the right approach but that both inputs should be combined in a global backcalculation process.

Finally, the experimental database will be enriched to confirm the previous results and sensitivity studies are planned, especially concerning the bituminous materials in situ temperature and the core-hole diameter. It is also intended to perform in situ tests on pavement section with well-known unbonded interfaces.

References

1. J.-M. Roussel, H. Di Benedetto, C. Sauzéat, and M. Broutin, "Spectral Element Simulation of Heavy Weight Deflectometer Test Including Layer Interface Conditions and Linear Viscoelastic Behavior of Bituminous Materials," in *Accelerated Pavement Testing to Transport Infrastructure Innovation*, ed. A. Chabot, P. Horny, J. Harvey, and L. G. Loria-Salazar (Cham, Switzerland: Springer Nature Switzerland AG, 2020), 658–665, https://doi.org/10.1007/978-3-030-55236-7_68
2. G. White, "Cyclic Shear Deformation of Asphalt at Melbourne Airport" (paper presentation, FAA Worldwide Airport Technology Transfer Conference, Galloway, NJ, August 5–7, 2014).
3. C. J. Bognacki, A. Frisvold, and T. Bennert, "Investigation of Asphalt Pavement Slippage Failures on Runway 4R-22L Newark International Airport" (paper presentation, FAA Worldwide Airport Technology Transfer Conference, Atlantic City, NJ, April 16–18, 2007).
4. A. Sadoun, M. Broutin, and J.-M. Simonin, "Assessment of HWD Ability to Detect Debonding of Pavement Layer Interfaces," in *Eighth RILEM International Conference on Mechanisms of Cracking and Debonding in*

- Pavements, ed. A. Chabot, W. G. Buttlar, E. V. Dave, C. Petit, and G. Tebaldi (Dordrecht, the Netherlands: Springer, 2016), 763–769, https://doi.org/10.1007/978-94-024-0867-6_106
5. M. Broutin, S. Fauchet, and D. Mounier, “A Full-Scale Instrumented Test-Facility for Airport Pavement Modeling Improvements,” in *Airfield and Highway Pavement 2013: Sustainable and Efficient Pavements*, ed. I. L. Al-Qadi and S. Murrell (Reston, VA: American Society of Civil Engineers, 2013), 1396–1408, <https://doi.org/10.1061/9780784413005.118>
 6. M. Broutin and A. Duprey, “Towards Improved Temperature Correction for NDT Data Analyses,” in *Airfield and Highway Pavements 2017: Design, Construction, Evaluation, and Management of Pavements*, ed. I. L. Al-Quadi, H. Ozer, E. M. Vélez-Vega, and S. Murrell (Reston, VA: American Society of Civil Engineers, 2017), 244–255, <https://doi.org/10.1061/9780784480922.022>
 7. C. Petit, A. Chabot, A. Destrée, and C. Raab, “Recommendation of RILEM TC 241-MCD on Interface Debonding Testing in Pavements,” *Materials and Structures* 51, no. 4 (July 2018): 96, <https://doi.org/10.1617/s11527-018-1223-y>
 8. C. Petit, A. Chabot, A. Destrée, and C. Raab, “Interface Debonding Behavior,” in *Mechanisms of Cracking and Debonding*, ed. W. G. Buttlar, A. Chabot, E. V. Dave, C. Petit and G. Tebaldi (Cham, Switzerland: Springer, 2018), 103–153, https://doi.org/10.1007/978-3-319-76849-6_3
 9. G. N. Savin, *Stress Concentration Around Holes*, 1st ed. (New York: Pergamon Press, 1961).
 10. R. Kobisch and C. Peyronne, “L’ovalisation: une nouvelle methode de mesure des deformations elastiques des chaussees,” *Bull Liaison Lab Ponts Chauss* 102 (July–August 1979): 59–71.
 11. M. Gharbi, M. Broutin, I. Boulkhemair, M. L. Nguyen, and A. Chabot, “Analysis of Ovalization Measurements on Flexible Airport Pavement under HWD Dynamic Impulse Load,” in *Proceedings of the RILEM International Symposium on Bituminous Materials – ISBM2020*, ed. H. Di Benedetto, H. Baaj, E. Chailleux, et al. (Cham, Switzerland: Springer, 2021), 263–269, https://doi.org/10.1007/978-3-030-46455-4_33
 12. O. Ruiz and G. Voisin, “L’essai d’ovalisation,” *RGRA* 962 (May 2019), <http://web.archive.org/web/20211123093513/> <https://www.editions-rgra.com/revue/962/auscultation/lessai-dovalisation>
 13. H. Goacolou, P. Keryell, R. Kobisch, and J. Poilane, “Utilisation de l’ovalisation en Auscultation des Chaussées,” *Bull Liaison Lab Ponts Chauss* 128 (November–December 1983): 65–75.
 14. J.-M. Martin, J.-P. Benaben, M. Jouaville, P. Lepert, J.-P. Poilane, C. Rapaud, and A. Simon, “Ovalisation, exécution et exploitation des mesures,” *Techniques et méthodes des laboratoires des Ponts et Chaussées - méthode d’essai LPC 41* (1995), http://web.archive.org/web/20211122195406/https://www.ifsttar.fr/fileadmin/user_upload/editions/lcpc/MethodeDEssai/MethodedeEssai-LCPC-ME41.pdf

15. M. Gharbi, M. Broutin, T. Schneider, S. Maindrout, and A. Chabot, “Towards an Adapted Ovalization System for Flexible Airfield Pavement Interface Characterization Using Rolling-Wheel or HWD Loads,” in *Accelerated Pavement Testing to Transport Infrastructure Innovation*, ed. A. Chabot, P. Hornych, J. Harvey, and L. G. Loria-Salazar (Cham, Switzerland: Springer, 2020), 516–525, https://doi.org/10.1007/978-3-030-55236-7_53
16. M. Broutin, A. Sadoun, and A. Duprey, “Comparison between HWD Backcalculated Subgrade Dynamic Moduli and In Situ Static Bearing Capacity Tests,” in *Airfield and Highway Pavements 2019: Design, Construction, Condition Evaluation, and Management of Pavements*, ed. I. Al-Qadi, H. Ozer, A. Loizos, and S. Murrell (Reston, VA: American Society of Civil Engineers, 2019), 404–413, <https://doi.org/10.1061/9780784482452.040>
17. M. Broutin and D. Mounier, “Release of the French Technical Guidance for Flexible Airfield Pavement Assessment Using HWD,” in *Airfield and Highway Pavements Pavement 2015: Innovative and Cost-Effective Pavements for a Sustainable Future*, ed. J. Harvey and K. F. Chou (Reston, VA: American Society of Civil Engineers, 2015), 330–341, <https://doi.org/10.1061/9780784479216.030>
18. M. Broutin, “Assessment of Flexible Airfield Pavements Using Heavy Weight Deflectometers. Development of a FEM Dynamical Time-Domain Analysis for the Backcalculation of Structural Properties” (PhD diss., Ecole Nationale des Ponts et Chaussées, 2010).

Appendix: Prototype Details

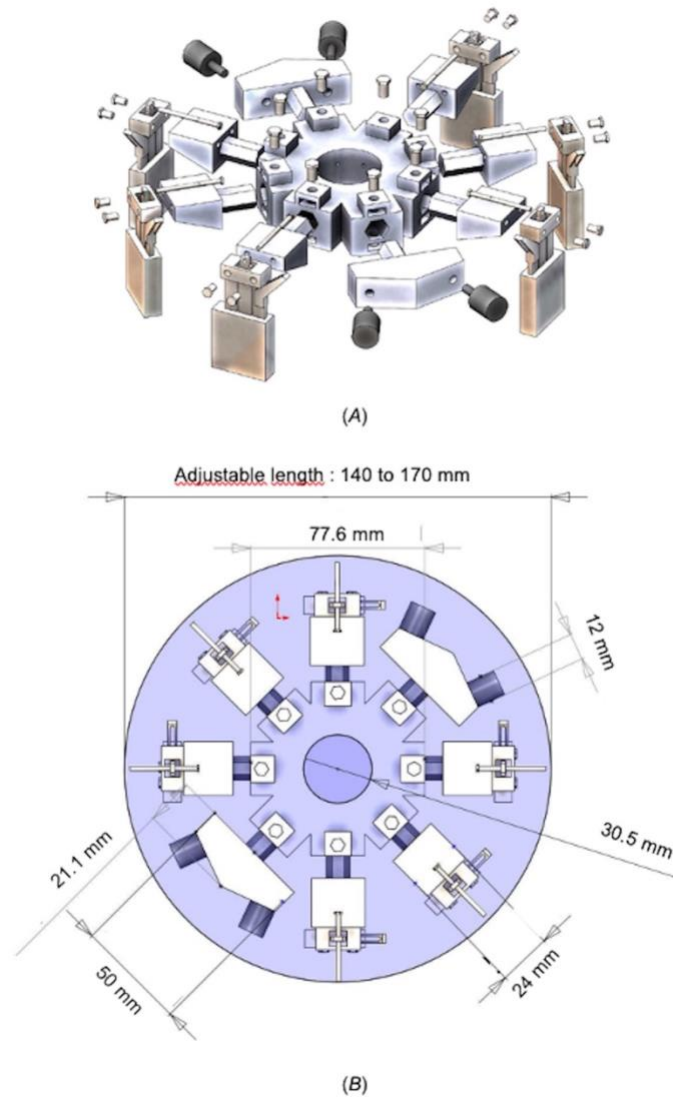


FIG. A.1 SolidWorks mechanical drawings of the ovalization device designed for a 162-mm diameter core-hole. (A) Exploded view and (B) XY view with dimensions.